Active Transport of an Antibiotic Rifamycin Derivative by the Outer-Membrane Protein FhuA

Andrew D. Ferguson,[1,2,3] Jiri Ködding,[1]
Georg Walker,[4] Christoph Bös,[4]
James W. Coulton,[3] Kay Diederichs,[1]
Volkmar Braun,[4] and Wolfram Welte[1,5]
[1] Fakultät für Biologie
Universität Konstanz
Konstanz D-78457
Germany
[2] Howard Hughes Medical Institute
Department of Biochemistry
University of Texas Southwestern Medical Center
Dallas, Texas 75390
[3] Department of Microbiology and Immunology
McGill University
Montréal, Québec H3A 2B4
Canada
[4] Lehrstuhl Mikrobiologie/Membranphysiologie
Universität Tübingen
Tübingen D-72076
Germany

Summary

Background: FhuA, an integral membrane protein of *Escherichia coli*, actively transports ferrichrome and the structurally related antibiotic albomycin across the outer membrane. The transport is coupled to the proton motive force, which energizes FhuA through the inner-membrane protein TonB. FhuA also transports the semi-synthetic rifamycin derivative CGP 4832, although the chemical structure of this antibiotic differs markedly from that of ferric hydroxamates.

Results: X-ray crystallography revealed that rifamycin CGP 4832 occupies the same ligand binding site as ferrichrome and albomycin, thus demonstrating a surprising lack of selectivity. However, the binding of rifamycin CGP 4832 is deviant from the complexes of FhuA with hydroxamate-type ligands in that it does not result in the unwinding of the switch helix but only in its destabilization, as reflected by increased B factors. Unwinding of the switch helix is proposed to be required for efficient binding of TonB to FhuA and for coupling the proton motive force of the cytoplasmic membrane with energy-dependent ligand transport. The transport data from cells expressing mutant FhuA proteins indicated conserved structural and mechanistic requirements for the transport of both types of compounds.

Conclusions: We conclude that the binding of rifamycin CGP 4832 destabilizes the switch helix and promotes the formation of a transport-competent FhuA-TonB complex, albeit with lower efficiency than ferrichrome. Active transport of this rifamycin derivative explains the 200-fold increase in potency as compared to rifamycin,

which is not a FhuA-specific ligand and permeates across the cell envelope by passive diffusion only.

Introduction

The uptake of antimicrobial agents across the outer membrane of gram-negative bacteria is mediated by a family of transport proteins employing a variety of mechanisms. Small hydrophilic solutes, primarily ions and sugars, are taken up into the periplasm by passive diffusion through nonspecific and substrate-specific porins. The structural architecture of bacterial porins, with their apparent exclusion limit of approximately 600 Da, and the electrostatic arrangement of charged side chains lining porin channels contribute to the exclusion of antibiotics from the cell interior [1]. When essential molecules ($>$600 Da) (including siderophores and vitamin B_{12}) are present at low concentrations, they are actively transported across the cell envelope. With the exception of the Donnan potential, no permanent electrical or chemical potential difference can be maintained across the outer membrane. Moreover, no source of energy has been localized in the periplasm. The chemical energy needed to drive these energy-dependent transport processes is provided by the electrochemical proton gradient maintained across the cytoplasmic membrane [2]. The energy-transducing TonB-ExbB-ExbD complex couples the proton motive force of the cytoplasmic membrane to a family of diverse outer-membrane proteins, the TonB-dependent transporters. In *E. coli*, the ferric hydroxamate uptake receptor FhuA actively transports the siderophores ferrichrome and ferricrocin, the cyclic peptide antibiotic microcin J25, the siderophore-antibiotic conjugate albomycin, and the bacterial toxin colicin M across the outer membrane [3]. FhuA also functions as the primary receptor for bacteriophages T1, T5, ϕ80, and UC-1.

The determination of the three-dimensional structure of FhuA was an important step toward understanding the intricate structure-function relationships of this receptor and its energy-dependent transport mechanism [4, 5, 7]. FhuA is composed of two domains; a 22 strand β barrel (residues 161–714) spans the outer membrane, and longer extracellular loops and shorter periplasmic turns connect adjacent, antiparallel transmembrane β strands. Part of the barrel interior is occluded by the cork domain, an amino-terminal globular domain (residues 1–160) composed of a mixed 4 strand β sheet and a series of short α helices. The residues that compose the ligand binding site are located within a nonoccluded portion of the β barrel, which is accessible from the external solvent.

FhuA possesses high affinity but limited structural specificity for hydroxamate-type siderophores including ferrichrome, a cyclic hexapeptide composed of three

[5] Correspondence: wolfram.welte@uni-konstanz.de

δ-*N*-acetyl-L-δ-*N*-hydroxyornithine and three glycine residues. Structural alteration of the iron-chelating portion of this siderophore abrogates receptor-specific recognition [6]. In contrast, structural analogs of ferrichrome that possess identical iron-chelating and distinct hydrophobic peptide linkers, including ferricrocin and albomycin, are bound and transported by FhuA. Because albomycin is actively transported across both the outer and cytoplasmic membranes, it is one of the most potent antibiotics against *E. coli* (minimal inhibitory concentration [MIC] of 0.005 μg/ml). The three-dimensional structure of FhuA in complex with albomycin [7] confirmed that this antibiotic occupies the same ligand binding site as ferrichrome, ferricrocin, and phenylferricrocin. This similarity extends to the set of residues that are involved in ligand binding and which are essentially conserved among these hydroxamate-type siderophores, and it thereby provides a structural explanation for high-affinity binding.

In 1987, Wehrli et al. [8] described a semisynthetic rifamycin derivative, CGP 4832, that displayed at least a 200-fold increase in antimicrobial activity against *E. coli* and *Salmonella typhimurium* as compared to the clinically used drug rifamycin (Rifampicin). The enhanced bactericidal activity of rifamycin CGP 4832 was correlated with the ability of this antibiotic to be specifically transported into the periplasm by FhuA [9]. In contrast to albomycin, rifamycin CGP 4832 is not actively transported across the cytoplasmic membrane by FhuBCD [9], which is an ABC transport system [10]. The periplasmic binding protein FhuD and the cytoplasmic membrane-embedded permease FhuBC effectively discriminate between rifamycin CGP 4832 and the diverse array of hydroxamate-type siderophores and antibiotics that are uniquely transported by this system [3]. Because the chemical structure of this rifamycin derivative shares no structural similarities with ferrichrome or with albomycin, we wished to determine how this antibiotic is specifically recognized and transported by FhuA. To establish whether it occupies the same ligand binding site as previously observed with hydroxamate-type siderophores and to characterize any distinct ligand-induced conformational changes, we determined the three-dimensional structure of FhuA in complex with rifamycin CGP 4832. Furthermore, we also studied the binding of ligands to FhuA by fluorescence measurements, transport inhibition, and selection of mutants resistant to this antibiotic. Our findings reveal common structural and mechanistic requirements for the energy-dependent transport of structurally dissimilar FhuA-specific ligands. Moreover, this structural information provides a basis for the rational design of synthetic antibiotics that are actively transported by this receptor or by its homologs. Because the outer membrane of gram-negative bacteria is inherently impermeable to polar substances >600 Da and therefore diffusional uptake is inefficient, such receptor-specific bactericidal agents may increase the efficacy of chemotherapeutic agents [7].

Results

General Description of the Structure and the Rifamycin CGP 4832 Binding Site

FhuA in detergent-containing solution was cocrystallized with rifamycin CGP 4832. Phases to 2.9 Å resolution

Table 1. Data Collection and Refinement Statistics of FhuA in Complex with Rifamycin CGP 4832

Data Collection and Reduction	
Space group	P6₁
Unit cell	
a (Å)	172.82
b (Å)	172.82
c (Å)	87.91
Number of molecules per asymmetric unit	1
Number of measured reflections	161,168
Number of unique reflections	33,363
Completeness (%)	99.9 (99.8)
Resolution (Å)	2.90
R_{sym} (%)	6.2 (29.8)
R_{meas} (%)	7.0 (33.5)
$R_{merge-F}$ (%)	7.2 (24.6)
$<I>/\sigma I$	17.2 (4.2)
Structural Refinement	
R_{work} (%)	23.3
R_{free} (%)	27.5
Root-mean-square deviation	
Bond lengths (Å)	0.008
Bond angles (°)	1.5
Dihedral angles (°)	25.9
Improper angles (°)	0.9
Mean B factor of the protein atoms (Å²)	68.0
Mean B factor of the ligand atoms (Å²)	98.7

Parentheses indicate the highest resolution shell.

were derived from the isomorphous, unliganded structure (Figure 1; Table 1; [4]). After initial structural refinement, a $F_{obs} - F_{calc}$ difference map showed clear electron density for a single rifamycin CGP 4832 molecule located within the extracellular pocket of FhuA (Figure
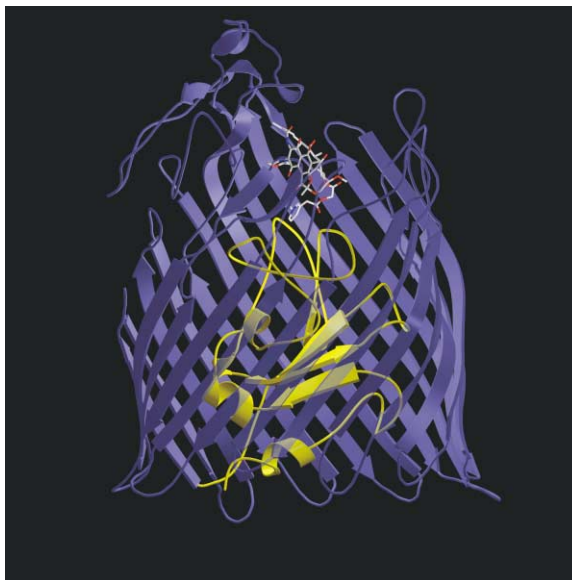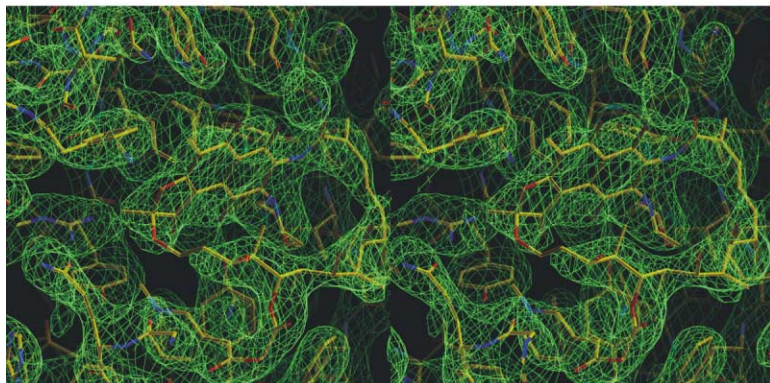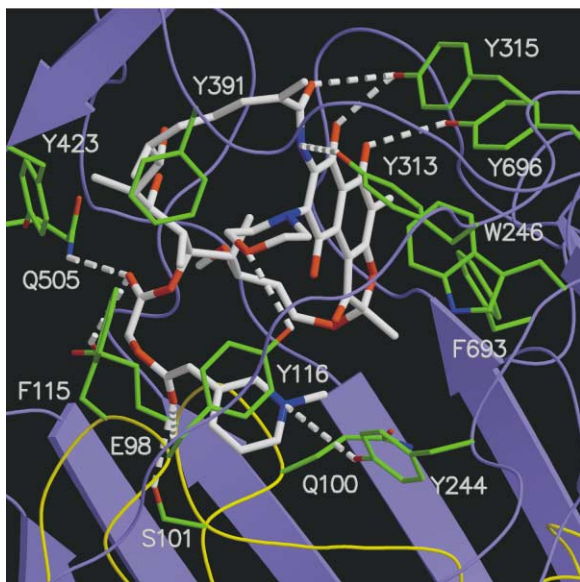

Figure 1. FhuA-CGP 4832 Complex

The view is perpendicular to the barrel axis. The β strands that form the front of the barrel domain have been rendered semitransparent; this provides an unobstructed view of the cork domain. The barrel domain is colored blue, and the cork domain is yellow. The rifamycin CGP 4832 molecule is shown as a bond model with carbon atoms in white, oxygen atoms in red, and nitrogen atoms in blue.

(a)

(b)

Figure 2. The FhuA Rifamycin CGP 4832 Binding Site

(a) Representative section of the electron density map for the FhuA-CGP 4832 complex. In this stereo view the final simulated annealing SIGMAA-weighted $2F_{obs} - F_{calc}$ map (green) at a resolution of 2.90 Å is contoured at 1.2 σ; this view shows the rifamycin CGP 4832 binding site. The rifamycin CGP 4832 molecule and select side chain residues are shown with carbon atoms in yellow, oxygen atoms in red, and nitrogen atoms in blue.

(b) The residues involved in the binding of CGP 4832. Those side chains that form hydrogen bonds or van der Waals contacts with rifamycin CGP 4832 atoms are labeled and shown in green. The rifamycin CGP 4832 molecule is presented as a bond model with carbon atoms in white, oxygen atoms in red, and nitrogen atoms in blue.

Figures 2a and 3 were prepared with the programs O [28] and ISIS Draw, respectively. All other color figures were prepared with MOLSCRIPT [33] and Raster3D [34].

2a). Side chains from apices B and C of the cork domain [4] and from the β barrel domain form hydrogen bonds, charge interactions, and van der Waals contacts with the antibiotic (Figures 2b and 3a; Table 2). The addition of morpholino and N-methyl-3-piperidyl-acetoxyacetyl groups structurally distinguishes rifamycin CGP 4832 from rifamycin; the latter is not actively transported by FhuA. Previous structure-function studies [8] demonstrated that both chemical moieties are required for the rifamycin derivative to exert its bactericidal activity. Our analysis of protein-ligand interactions between FhuA and rifamycin CGP 4832 showed that the morpholino and N-methyl-3-piperidyl-acetoxyacetyl groups form multiple hydrogen bonds, charge interactions, and van der Waals contacts with FhuA side chains (Figures 2b and 3a; Table 2). Chemical replacement of the morpholino moiety by a methyl-piperazinyl-iminomethyl substituent abolished the bactericidal activity of rifamycin CGP 4832 [9]. The structure indicated that substitution of the morpholino group would prevent the formation of a critical hydrogen bond between rifamycin CGP 4832 and Y116 from apex C and would thereby abrogate high-affinity binding.

Structural Comparison of the Ligand Binding Sites of FhuA

The chemical structure of rifamycin CGP 4832 (Figure 3a) shows no obvious similarity with albomycin (Figure 3b) and ferricrocin (Figure 3c). Moreover, the cork domain structure in the FhuA-CGP 4832 complex differs from that found in complexes with hydroxamate-type siderophores and albomycin. By comparing the side chains involved in the binding of these structurally dissimilar substrates, we identified signature residues that are involved in ligand binding (Table 3). The iron-chelating moiety of FhuA-specific hydroxamate-type siderophores and albomycin is formed by three δ-*N*-acetyl-L-δ-*N*-hydroxyornithine peptides. This portion of the siderophore forms multiple highly conserved interactions with side chains from apices A, B, and C of the cork domain, as well as with residues from the β strands and extracellular loops of the barrel domain (Figures 3b and 3c). There are also contacts between the tripeptide component of the siderophore (GGG [ferrichrome], GSG [ferricrocin], GFG [phenylferricrocin]) and the amino acetyl thioribosyl pyrimidine moiety of albomycin, with side chains of the extracellular pocket (Table 3). A similar set

Table 2. Interactions of FhuA with Rifamycin CGP 4832

Residue Atom	Location	Distance	Type of Interaction
E98-OE2	Apex B	3.7 Å	charge interactions with O8 carbonyl atom of the N-methyl-3-piperidyl-acetoxyacetyl group
E98-O	Apex B	3.8 Å	charge interactions with O20 carbonyl atom of the N-methyl-3-piperidyl-acetoxyacetyl group
G99-NH	Apex B	3.7 Å	charge interactions with O20 carbonyl atom
Q100-OE1	Apex B	3.5 Å	Van der Waals contact with the C5 methyl group
S101-OG	Apex B	3.5 Å	Hydrogen bond with O20 carbonyl atom
F115-O	Apex C	3.0 Å	Van der Waals contact with C55 atom of the piperidyl group
Y116-OH	Apex C	3.2 Å	hydrogen bond with O18 atom of the morpholino group
Y244-OH	L3	3.9 Å	charge interactions with N6 atom
W246-CZ2	L3	3.6 Å	Van der Waals contact with the aromatic-ring system (distance given is for the O17 atom)
Y313-OH	β7	3.6 Å	charge interactions with N4 atom
Y315-OH	L4	2.8 Å	hydrogen bond with O1 carbonyl atom of the aromatic-ring system
K344-CD	β8	3.4 Å	Van der Waals contact with C24 methyl group
F391-CE2	β9	3.0 Å	Van der Waals contact with O18 atom of the morpholino group and the C31 and C32 methyl groups
G392-O	β9	3.2 Å	Van der Waals contact with C24 methyl group
Y423-OH	β10	3.3 Å	Van der Waals contact with the C31 and C32 methyl groups
Q505-NE2	L7	3.0 Å	hydrogen bond with the O8 carbonyl atom of the N-methyl-3-piperidyl-acetoxyacetyl group
F693-CE1	L11	3.5 Å	Van der Waals contact with the aromatic-ring system (distance given is for C40 atom)
Y696-OH	L11	3.0 Å	hydrogen bond with O2 hydroxyl atom

Listed are the residue atoms, locations, distances, and types of interactions formed by all FhuA side chain residues within 4 Å of rifamycin CGP 4832. See Figure 3a for structural details of the hydrogen bonding pattern and charge interactions between side chains and rifamycin CGP 4832.

of side chains also forms contacts with rifamycin CGP 4832. However, there is one notable exception: R81 from apex A does not interact with the antibiotic. In the binding site for hydroxamate-type ligands, this residue forms multiple hydrogen bonds with the iron-chelating component of the siderophore. In the FhuA-CGP 4832 complex, the guanidinium group of R81 is placed 4.6 Å away from the nearest rifamycin CGP 4832 atom and thus forms only weak charge interactions with the derivative.

Ligand-Induced Allosteric Transitions

Structural superposition of the $C\alpha$ atoms of unliganded FhuA and FhuA liganded with rifamycin CGP 4832, ferrichrome, ferricrocin, phenylferricrocin, or albomycin revealed almost perfect superposition of the β barrel domains (0.25 Å root-mean-square deviation of $C\alpha$ atoms). However, a comparison of the $C\alpha$ atoms of the cork domain identified three distinct conformations: the hydroxamate-type unliganded, the liganded, and the CGP 4832-liganded conformations. The transition from the unliganded to the hydroxamate-type liganded conformation reveals the following induced-fit binding mechanism [4, 5, 7]: residues 80–82 of apex A and 98–100 of apex B moved by 0.7–2.0 Å toward the siderophore or albomycin. In the transition to the CGP 4832-liganded conformation, only residues 97–100 from apex B moved upward (0.5–1.5 Å) to interact with the antibiotic (Table 2). All other cork domain residues remained stationary. In the complexes with iron-hydroxamates, the upward translation of apex A is propagated to all cork domain loops between this point and the periplasmic pocket of FhuA. The translation of apex A and other cork domain loops alters the shape of the hydrophobic pocket of the switch helix (residues 24–29), disrupts several hydrogen

bonds formed between periplasmic turns 8 and 9 and this helix and thereby promotes its unwinding. As a result, all residues NH_2-terminal of R31 assume an extended conformation within the periplasmic pocket. In contrast, apex A in the FhuA-CGP 4832 complex remains fixed 4.6 Å away from the nearest ligand atom, as in the unliganded conformation. No upward movement of this cork domain loop is induced, and therefore the switch helix remains wound. However, the increase in relative B factors of the $C\alpha$ atoms composing the switch helix suggests that this segment is destabilized when rifamycin CGP 4832 binds (Figure 4). The allosteric transition induced by this antibiotic thus differs from those observed with other liganded complexes of FhuA.

To confirm these unexpected crystallographic observations, we collected intrinsic tryptophan fluorescence measurements with detergent-solubilized FhuA. In accord with Locher and Rosenbusch [11], we found that the addition of ferrichrome to purified, detergent-solubilized FhuA decreased the emitted intrinsic tryptophan fluorescence of the receptor. A slight decrease in tryptophan fluorescence upon the binding of rifamycin CGP 4832 or desferriferrichrome was also observed (Figure 5a). Unexpectedly, the addition of ferrichrome to a tryptophan solution of equivalent concentration also decreased the emitted fluorescence (Figure 5b). However, the magnitude of the fluorescence quenching was not equivalent to that observed with FhuA. The addition of rifamycin CGP 4832 or desferriferrichrome to the tryptophan solution also failed to produce a similar effect (Figure 5b).

A second biophysical method for monitoring ligand-induced structural transitions in FhuA was provided by the measurement of fluorescence changes of fluores-

(a)
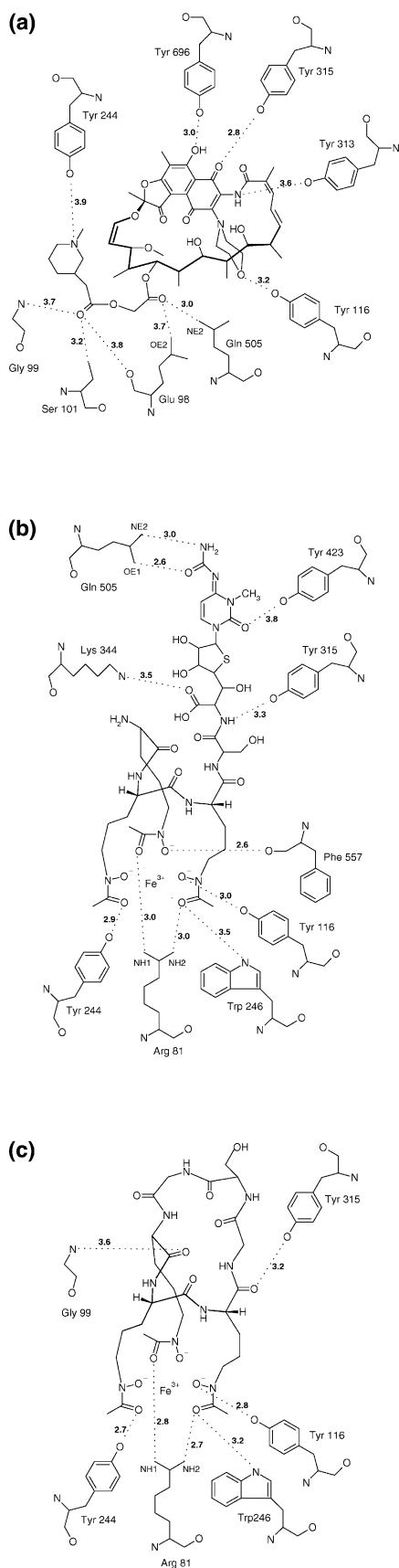
cein-labeled cysteine residues. This technique has advantages in that the location of the reporter is known and in that data can be collected directly from viable, intact cells. It was shown previously [12] that ferrichrome binding to FhuA quenched the emitted fluorescence of two fluorescein-labeled cysteines, residues 329 and 336, which are located in the fourth extracellular loop according to the three-dimensional structure of FhuA. Rifamycin CGP 4832 binding caused a similar reduction in fluorescence of both surface-exposed cysteines. However, a 100-fold higher concentration of rifamycin CGP 4832 was required to obtain a similar ferrichrome bound spectrum (Table 4). The observed fluorescence quenching by rifamycin CGP 4832 was not a function of the TonB-dependent transport of this antibiotic through FhuA since identical spectra were obtained from *tonB*-deleted background strains (data not shown). The binding of ferrichrome to FhuA also induced a similar TonB-independent shift in fluorescence [12].

Rifamycin CGP 4832 Competes with Ferrichrome for Binding to the Ligand Binding Site of FhuA

To probe the functional implications resulting from the similarity of the binding sites for rifamycin CGP 4832 and ferrichrome, we performed transport inhibition assays. The addition of 10, 30, or 100 μg/ml of rifamycin CGP 4832 produced a 50%, 75%, or 85% reduction in the $[^{55}Fe^{3+}]$-ferrichrome transport rate (Figure 6). These data indicate that this antibiotic competes with ferrichrome for the same binding site and that both substrates have similar binding affinities. Because rifamycin CGP 4832 does not use the FhuBCD ferrichrome transport system across the cytoplasmic membrane, competitive transport inhibition is confined to passage across the outer membrane only [9].

Bacterial Mutants Resistant to Rifamycin CGP 4832

To determine if the energy-dependent transport of rifamycin CGP 4832 and ferrichrome share common structural requirements, we assessed the sensitivity for the antibiotic of cells expressing FhuA proteins with known point mutations in their TonB boxes (residues 6–11); these mutations all exhibit impaired TonB-related FhuA activity [13]. Plasmid-encoded *fhuA* genes were used to transform *E. coli* UL3, which does not synthesize a wild-type FhuA protein. In contrast to cells expressing wild-type FhuA, those producing FhuA mutants I9P or V11D showed resistance to 0.4–10 μg/ml of rifamycin CGP 4832. The antibiotic sensitivity of mutant and wild-type cells for rifamycin CGP 4832 and rifamycin were

(b)

(c)

Figure 3. Ligand Binding to FhuA

Schematic comparison of the hydrogen bonding pattern and charge interactions of the side chain residues of the FhuA ligand binding site with (a) rifamycin CGP 4832, (b) albomycin (extended conformational isomer) [7], and (c) ferricrocin [4]. The chemical structures of ferricrocin, albomycin, and rifamycin CGP 4832 are shown with hydrogen bonds and charge interactions with side chains as dotted lines (distances are given in Å). Hydrogen atoms have been partly omitted. See Table 2 for details of additional van der Waals contacts between side chains and rifamycin CGP 4832.

Table 3. Interactions of FhuA with its Cognate Ligands Bound to the Extracellular Pocket

Side Chain Residues	Ferricrocin	Phenylferricrocin	Albomycin*	Albomycin†	Rifamycin CGP 4832
R81 from apex A	+	+	+	+	−
Y87 from a cork domain loop	−	+	−	−	−
E98 near apex B	−	−	−	−	+
G99 near apex B	+	+	+	+	+
Q100 from apex B	+	+	+	+	+
S101 from a cork domain loop	−	−	−	−	+
F115 near apex C	−	+	−	+	+
Y116 from apex C	+	+	+	+	+
Y244 from L3	+	+	+	+	+
W246 from L3	+	+	+	+	+
Y313 from β7	+	+	+	+	+
Y315 from L4	+	+	+	−	+
K344 from β8	−	−	+	−	+
F391 from β9	+	+	+	+	+
G392 from β9	−	−	−	−	+
Y393 from L5	−	−	+	+	−
Y423 from β10	−	−	−	+	+
Q505 from L7	−	−	−	+	+
F557 from L8	−	−	+	−	−
F558 from L8	−	−	+	−	−
F693 from L11	+	+	+	+	+
Y696 from L11	−	−	−	−	+

Listed are all side chains within 4 Å of ligand atoms: ferricrocin [4]; phenylferricrocin [7]; albomycin extended (*) and compact (†) conformational isomers [7]; and rifamycin CGP 4832.

equivalent at high concentrations (>100 µg/ml); the latter compound is not actively transported by FhuA and presumably permeates through the outer membrane by passive diffusion only.

Discussion

Ligand Binding and Concomitant Allosteric Conformational Transitions

In contrast to rifamycin, the semisynthetic derivative CGP 4832 binds to FhuA. Competition of ferrichrome transport by CGP 4832, as shown in this paper, indicates a common binding site for both substrates, and the
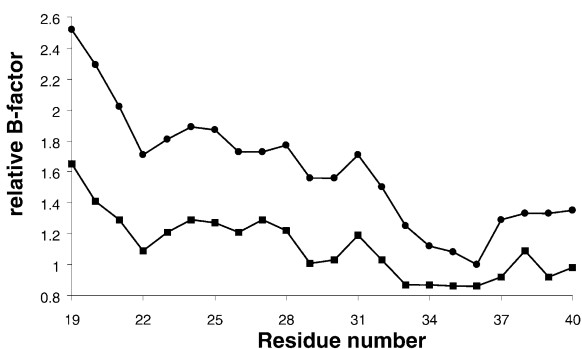

Figure 4. Destabilization of the Switch Helix upon Binding of CGP 4832

Relative B factors of the first 21 C_α atoms of unliganded FhuA (closed square) and FhuA liganded with the rifamycin CGP 4832 (closed circle). Relative B factors are B factors divided by the mean B factor of all C_α atoms of the respective structure; the mean B factor for unliganded FhuA is 63 Å^2 (σ = 13.6) and for FhuA in complex with rifamycin CGP 4832 is 68 Å^2 (σ = 14.0). Residues 24–29 compose the switch helix.

concentration dependence of CGP 4832 inhibition suggests a rather high affinity of CGP 4832 to FhuA (K_D for ferrichrome is <0.1 µM [3]). It was mere coincidence that screening rifamycin derivatives against *E. coli* and related gram-negative bacteria identified this antibiotic, which fits snugly into the common binding site of FhuA and is actively transported across the outer membrane. The crystal structure of FhuA in complex with rifamycin CGP 4832 showed that high-affinity binding results from the addition of morpholino and N-methyl-3-piperidyl-acetoxyacetyl moieties to rifamycin. These additional groups form most of the specific interactions with side chains found in the extracellular pocket of FhuA. Most transport proteins display high affinity for their cognate ligands; however, they rarely covalently modify their substrates and thereby impose stringent geometric constraints on those side chains lining the binding site. For this reason, transporters tolerate larger structural diversity than enzymes, as observed in the FhuA-CGP 4832 complex.

The binding of ferrichrome or albomycin to FhuA induces a short NH$_2$-terminal segment designated the switch helix (residues 24–29) to unwind and thus displace E19 approximately 17 Å from its unliganded C_α position to a site designated the "putative channel-forming segment" [4, 5, 7]. These crystallographically determined TonB-independent conformational transitions are in accord with in vivo and in vitro data collected from intact cells and from detergent-solubilized FhuA. Specifically, ligand binding reduced the efficiency of the binding of monoclonal antibodies that are sensitive to the conformation of residues 21–59 [14], enhanced the formation of a chemically crosslinked FhuA-TonB complex [15], decreased the intrinsic tryptophan fluorescence of FhuA [11], and caused fluorescence quenching of fluorescein-maleimide bound to a genetically intro-

duced cysteine residue in the fourth extracellular loop [12]. The translation of W22 (which in unliganded conformation is buried together with the switch helix within a hydrophobic pocket) by approximately 17 Å across the periplasmic pocket of FhuA upon the binding of hydroxamate-type siderophores or albomycin may substantially contribute to tryptophan quenching.

FhuA in complex with rifamycin CGP 4832 possesses a conformation that lies between the unliganded and hydroxamate bound conformations of FhuA. Apex B moves upward to the antibiotic and causes a similar relocation of the neighboring cork domain segments, as observed with hydroxamate-type ligands. In contrast to the hydroxamate-bound conformation of FhuA, apex A does not interact with rifamycin CGP 4832; thus, the switch helix remains wound in the CGP 4832-liganded conformation. Nevertheless, the movement of apex B does allosterically affect the hydrophobic pocket in which the switch helix resides, as judged from the increase in relative B factors of the C_α atoms. This suggests that the switch helix may temporarily unwind, albeit with lower probability than in the hydroxamate type-liganded conformation.

Interaction of TonB with FhuA and the Functional Consequences

The pronounced allosteric transition observed in hydroxamate-type ligand binding presumably serves to recruit the energy-transducing protein TonB to the TonB box, its principal site of known interaction with TonB-dependent transporters. Relocation of this highly conserved segment is likely required for efficient coupling of TonB with FhuA. This NH_2-proximal region of FhuA is localized in the periplasm and has been shown by genetic and biochemical means to interact physically with a region of TonB at or near residue 160 [13, 16]. The failure to visualize this segment of FhuA (residues 6–11) in any of the currently available electron density maps [4, 5, 7] agrees with its apparent flexibility. However, the solution of the three-dimensional structure of the ferric enterobactin receptor FepA [17] revealed that the TonB box assumes an extended structure.

Direct physical interactions between the TonB box of the outer-membrane vitamin B_{12} transporter BtuB and a segment of TonB around residue 160 have been demonstrated by in vivo disulphide crosslinking [18]. Site-directed spin labeling and electron paramagnetic resonance assays have also indicated that in the unliganded conformation the TonB box of BtuB may be localized adjacent to a helix that forms specific interactions with side chain residues from the periplasmic turns of the β barrel domain of the receptor [19]. The binding of vitamin B_{12} converted this segment into an extended, disordered, and highly dynamic structure that likely extends into the periplasm to interact physically with TonB. Collectively, these findings support the proposal that the unwinding of the switch helix promotes the formation of the FhuA-TonB complex in vivo, and this may be an essential mechanistic requirement for the coupling of the proton motive force of the cytoplasmic membrane with receptor-mediated ligand transport across the outer membrane.
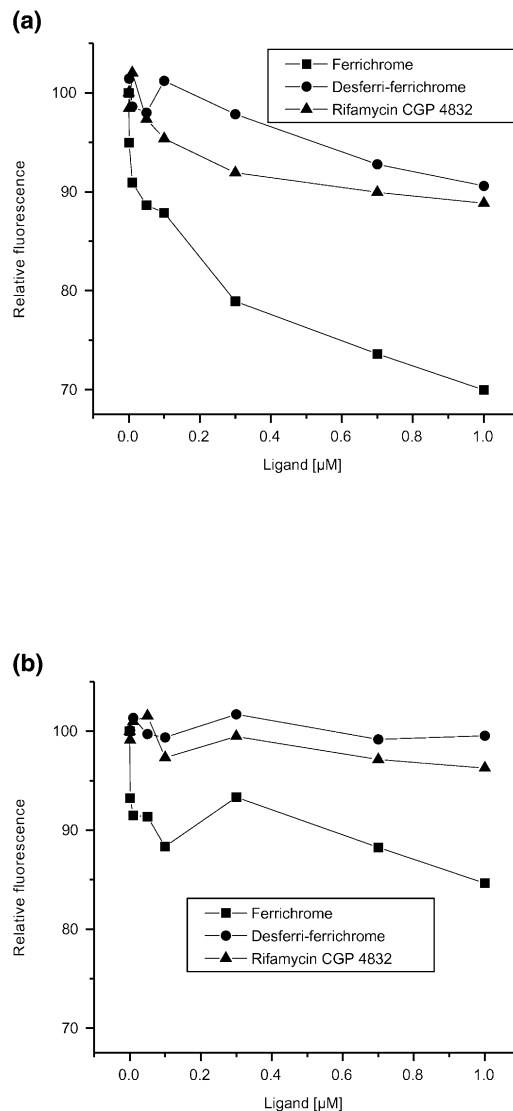

Figure 5. Ligand-Induced Fluorescence Quenching

Tryptophan fluorescence of solutions containing (a) FhuA and (b) tryptophan is shown for ferrichrome (closed square), desferriferrichrome (closed circle), and rifamycin CGP 4832 (closed triangle). The given tryptophan fluorescence values were averaged from three independent experiments in which each spectrum was collected three times. The background fluorescence spectra of all buffers (without added ligand) were subtracted from the collected experimental spectra. The emitted tryptophan fluorescence of FhuA was taken as 100%.

Given the TonB dependence of rifamycin CGP 4832 transport as shown in [9] and the data presented here, FhuA may assume two conformations that are in equilibrium. The majority of FhuA molecules have wound switch helices, while a small fraction contain unwound switch helices. Under crystal growth conditions, this equilibrium may be skewed toward the helical conformation; however, in vivo a small percentage of FhuA proteins may be sufficient for the formation of transport-competent complexes with TonB and may thereby sustain the observed transport rate. Alternatively, the physical interaction of TonB with the destabilized switch helix may

Table 4. Ligand-Induced Fluorescence Quenching of Fluorescein-Maleimide-Labeled Cells

FhuA	Not Preincubated with CGP 4832	Preincubated with 1 μM CGP 4832	−ΔF (%)	Not Preincubated with Ferrichrome	Preincubated with 10 nM Ferrichrome	−ΔF (%)
Wildtype	16.6	16.5	0	16.2	16.3	0
C329S (C318)	25.9	23.9	8	26.4	24.0	9
C318S (C329)	43.3	34.1	21	43.1	33.7	22
D336C	94.7	62.7	34	94.3	70.7	26

E. coli UL3 cells expressing the plasmids pfhuA4 (C318S), pfhuA5 (C329S), pfhuA6 (D336C), and pfhuA8 (wild-type FhuA) were labeled as described previously [12]. Mean relative fluorescence value prior to and following preincubation with 1 μM rifamycin CGP 4832 or 10 nM ferrichrome are shown. −ΔF (%) indicates the ligand-induced decrease in relative fluorescein-maleimide labeling for cells not preincubated with 1 μM rifamycin CGP 4832 or 10 nM ferrichrome [σ (n − 1) = 10%].

allow for an induced fit and yield a productive complex at a sufficient rate. Finally, the direct physical interaction of the TonB box of FhuA with TonB may not be essential for the transport of rifamycin CGP 4832; this would indicate the presence of at least one additional site of interaction between FhuA and TonB. The latter interpretation is supported by the finding that removing the entire cork domain from the β barrel (including the TonB box) generates a mutant FhuA protein (FhuAΔ5-160) with residual TonB-dependent transport activity, including the uptake of rifamycin CGP 4832 [20]. When the cork domain is genetically excised, interactions between TonB and the barrel domain of FhuA may be sufficient for the induction of a structural transition within the barrel such that the ligand is released from its residual binding site [20]. To further probe the functional role of the TonB box in the transport of rifamycin CGP 4832, we assessed a series of bacterial strains with known point mutations in their TonB boxes [13]; all FhuA-mediated, TonB-dependent transport activities were impaired in these strains. The sensitivities of these cells to the bactericidal effects of rifamycin CGP 4832 were equivalent to the

bactericidal effects of rifamycin that is not actively transported by FhuA but instead presumably permeates through the outer membrane by passive diffusion only. These genetic data indicate that the conformation of the TonB box and its physical interaction with TonB are involved in the uptake of rifamycin CGP 4832.

A Proposed Transport Mechanism

For integrating the available biochemical, genetic, and structural data, we propose the following model of TonB-dependent ligand transport. First, the binding of the hydroxamate-type siderophores or albomycin to the extracellular pocket of FhuA causes a TonB-independent conformational change. This change is propagated through the outer membrane and displayed by select periplasmic segments of the receptor, primarily the switch helix and the TonB box. The unwinding of the switch helix and the accompanying translocation (or possibly a change in the conformation) of the TonB box, alone or in combination with conformational changes of periplasmic segments, may serve to recruit TonB to its site of interaction with FhuA.

Upon forming a productive complex with FhuA, TonB transduces conformational energy to the transporter. This event triggers a TonB-dependent conformational change in FhuA such that the ligand binding site is disrupted and the binding affinity is reduced. Disruption of the binding site may be affected by a small shift of apices A, B, and C toward the periplasm. This may transiently alter the arrangement of the aromatic side chain residues lining the extracellular pocket, specifically those found on the fourth extracellular loop [12]. Furthermore, the transduction of energy causes a high-conductance channel to open within FhuA. This channel may be physically and electrically similar to that formed upon the irreversible adsorption of bacteriophage T5 to FhuA, as mediated by the straight tail fiber protein pb5 [21, 22]. Although the open-channel conformation of FhuA remains to be determined structurally, we speculate that subtle conformational changes in the loops of the cork domain between apex B and the periplasmic pocket may be involved in channel formation. When viewed along the barrel axis of unliganded FhuA and its liganded complexes, the extracellular pocket is connected to the periplasmic pocket in one segment (the putative channel-forming segment) of the barrel cross-section by a 10 Å aqueous channel. Once released from their binding sites, ligands may enter this region and reach the periplasmic pocket by directed diffusion along a string of
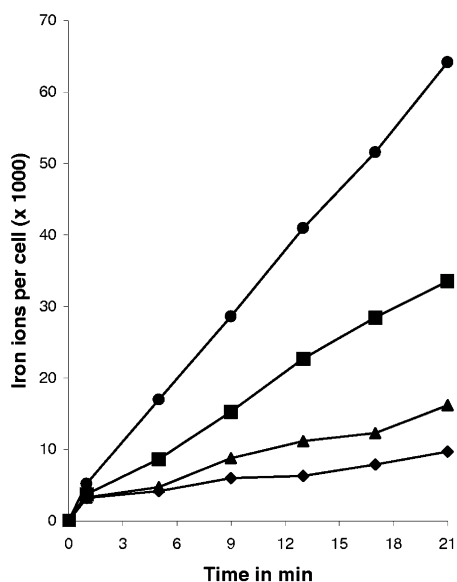

Figure 6. Transport Inhibition Assays with Rifamycin CGP 4832

Transport of radiolabeled [$^{55}Fe^{3+}$]-ferrichrome (2.35 μM) into *E. coli* AB2847 cells in the absence (closed circle) and presence of 10 μg/ml (closed square), 30 μg/ml (closed triangle), and 100 μg/ml (closed diamond) of rifamycin CGP 4832.

low-affinity binding sites. These transient ligand binding sites could be provided by a set of strictly conserved side chain residues lining the interior barrel wall of the putative channel-forming segment from the ligand binding site to the periplasmic pocket of FhuA [4, 23].

The observed switch helix destabilization when rifamycin CGP 4832 binds suggests that the helix may briefly unwind or allow complex formation with TonB by an induced-fit mechanism at a low rate. We suggest that this small yield of productive complexes among the rifamycin CGP 4832-loaded FhuA molecules may establish the transport of antibiotic molecules across the outer membrane at a rate sufficient to inhibit RNA polymerase activity [24]. Collectively, these results provide a structural basis for the superior bactericidal activity of CGP 4832 against *E. coli* (MIC of 0.02 μg/ml) as compared to that of rifamycin (MIC of 4.0 μg/ml).

Evolution of TonB-Dependent Receptors

Bacterial cells that synthesize the deletion derivative FhuAΔ5-160 retain a diminished level of TonB-dependent activity [20], and this finding suggests that the barrel domain together with TonB can constitute a functional transport system. We therefore speculate that ancient gram-negative bacteria possessed a channel-forming protein similar to FhuAΔ5-160. A string of low-affinity binding sites spanning the outer membrane may have facilitated the uptake of iron-containing siderophores, as observed with glycoporin-mediated carbohydrate uptake [25, 26].

Biological Implications

Transport proteins bind their freight molecules with high affinity in order to achieve a high transport rate in situations where molecules are available at low concentrations only. Moreover, they avoid high selectivity in order to transport a broad range of molecules. Transport systems therefore can be cheated by molecular mimicry. Our work has revealed structural and mechanistic details of how a molecule which is rather different in its chemical structure from natural substrates can be actively transported and thus act as an antibiotic at a very low dose. We predict that in the struggle among organisms such mimicry occurs quite often, and that this principle may guide researchers in the rational development of new antibiotics.

Experimental Procedures

Crystallization, Data Collection, and Structure Determination
Using the hanging drop vapor diffusion technique, we cocrystallized FhuA with rifamycin CGP 4832 by mixing equal volumes (5 μl) of FhuA (10 mg/ml, 0.80% N,N-dimethyldecylamine-N-oxide [DDAO], 10 mM ammonium acetate [pH 8.0], 1% *cis*-inositol, and 1 mM rifamycin CGP 4832) and reservoir solution (12% polyethylene glycol [PEG] 2000 monomethyl ether, 0.1 M sodium cacodylate [pH 6.4], 20% glycerol, and 3% PEG 200). Rifamycin CGP 4832 was generously provided by Dr. Reto Naef (Novartis-Pharma, Switzerland). FhuA-CGP 4832 cocrystals grew within seven days to a final size of 300 × 300 × 220 μm at 18°C. Crystals were mounted in cryoloops and flash frozen by direct immersion into liquid nitrogen. Diffraction data were collected at 100 K by the use of a cryostream apparatus with synchrotron radiation at the X-ray diffraction beam line at the Elettra synchrotron (Trieste, Italy) (Table 1). X-ray diffraction data

were processed and reduced with the program XDS [27]. Initial phases for the FhuA-CGP 4832 complex were calculated with the FhuA coordinates (1QFG) as an initial model. A model for the FhuA-CGP 4832 complex was built into an experimental electron density map with the program O [28]. The model was refined with the program CNS by the use of molecular dynamics and the maximum-likelihood target [29]. After rounds of model building and structural refinement, the final model contained residues 19–714, 1 lipopolysaccharide molecule, 1 rifamycin CGP 4832 molecule, 1 DDAO molecule, and 178 ordered water molecules.

Isolation and Characterization of Rifamycin CGP 4832-Resistant Bacterial Mutants
To assess the sensitivity of defined FhuA mutants to rifamycin CGP 4832, we used *E. coli* UL3 [12] that was transformed with plasmid-encoded *fhuA* genes with point mutations in their TonB boxes [13]. Plasmid pHK763 encoding wild-type FhuA served as a control. Wild-type and mutant *fhuA* genes were cloned on the same pT7-5 plasmid. Aliquots (20 μl) of a 10-fold dilution series of rifamycin CGP 4832 (stock solution: 0.5 mg in 1 ml of 50% methanol) and rifamycin were spotted in parallel onto nutrient agar plates seeded with 10^8 cells of *E. coli* UL3. Diameters of the zones of growth inhibition were recorded.

Transport Inhibition Assays with Rifamycin CGP 4832
E. coli AB2847 cells were grown overnight on TY nutrient agar plates. This *E. coli* strain has a mutation in *aroB,* a gene required for the synthesis of enterobactin, the only endogenous siderophore. If appropriate precursors are not provided, *E. coli* AB2847 will transport exogenously added siderophores. Colonies were suspended in 0.5 ml of M9 minimal media salts supplemented with 0.4% glucose and grown to an optical density of 0.55 at 578 nm [30]. Nitrilotriacetate (8.8 μl of a 10 mM solution) was added to 0.35 ml of cell suspension. After a 2 min incubation period, 3.5 μl aliquots of rifamycin CGP 4832 (1, 3, and 10 mg/ml dissolved in 50% methanol) were added to the cell culture. After an additional 3 min, transport was initiated by the addition of a mixture of 2.35 μM radiolabeled [$^{55}Fe^{3+}$]-ferrichrome and 5 μM desferriferrichrome. The cell suspension was shaken, and 50 μl samples were withdrawn after 1 and 4 minute intervals, for a total of 21 min. The samples were subsequently filtered, washed twice with 5 ml of 0.1 M LiCl, and dried, and the [$^{55}Fe^{3+}$]-isotope signal was measured with a liquid scintillation counter at 37°C. *E. coli* UL3 does not synthesize a wild-type FhuA protein, and there is no polar effect on the expression of the *fhuCDB* genes, which are located downstream of *fhuA.*

Protein Expression, Purification, and Intrinsic Tryptophan Fluorescence Measurements
A recombinant FhuA protein was constructed by the insertion of a hexahistidine tag plus five additional linker residues (SSHHHHHHGSS) after residue 405 in the *fhuA* gene [31]. FhuA was expressed and purified as previously described [32]. The intrinsic tryptophan fluorescence of FhuA and its complexes with rifamycin CGP 4832, with ferrichrome, or with desferriferrichrome (dissolved in 6 mM KH$_2$PO$_4$ [pH 7.0], 0.15 M NaCl, and 0.06% N,N-dimethyldodecylamine-N-oxide) were measured in 1.1 μM FhuA solutions and, as a control, in 10 μM tryptophan solutions. FhuA ($\sim$79 kDa with 9 tryptophan residues) (1.1 μM) was considered equivalent to a 10 μM tryptophan solution. All data were collected at 20°C with a Fluoromax-2 spectrophotometer (Jobin Yvon-Spex Instruments) and processed with the GRAMS/386 software package. A single excitation wavelength (280 nm) was used for all fluorescence measurements. Two emission wavelengths were collected, and they correspond to the fluorescence maxima of FhuA (335 nm) and tryptophan (355 nm).

References

1. Welte, W., Nestel, U., Wacker, T., and Diederichs, K. (1995). Structure and function of the porin channel. Kidney Int. *48*, 930–940.
2. Bradbeer, C. (1993). The proton motive force drives outer membrane transport of cobalamin in *Escherichia coli*. J. Bacteriol. *175*, 3146–3150.
3. Braun, V., Hantke, K., and Köster, W. (1998). Bacterial Iron Transport: Mechanisms, Genetics, and Regulation. In Iron Transport and Storage in Microorganisms, Plants, and Animals, volume 35, A. Sigel and H. Sigel, eds. (New York: Marcel Dekker Inc.), pp. 67–145.
4. Ferguson, A.D., Hofmann, E., Coulton, J.W., Diederichs, K., and Welte, W. (1998). Siderophore-mediated iron transport: crystal structure of FhuA with bound lipopolysaccharide. Science *282*, 2215–2220.
5. Locher, K.P., et al., and Moras, D. (1998). Transmembrane signalling across the ligand-gated FhuA receptor: crystal structures of free and ferrichrome-bound states reveal allosteric changes. Cell *95*, 771–778.
6. Jurkevitch, E., Hadar, Y., Chen, Y., Libman, J., and Shanzer, A. (1992). Iron uptake and molecular recognition in *Pseudomonas putida*: receptor mapping with ferrichrome and its biomimetic analogs. J. Bacteriol. *174*, 78–83.
7. Ferguson, A.D., et al., and Welte, W. (2000). Crystal structure of the antibiotic albomycin in complex with the outer membrane transporter FhuA. Protein Sci. *9*, 956–963.
8. Wehrli, W., et al., and Zak, O. (1987). CGP 4832, a semisynthetic rifamycin derivative highly active against some Gram-negative bacteria. J. Antibiot. *40*, 1733–1739.
9. Pugsley, A.P., Zimmerman, W., and Wehrli, W. (1987). Highly efficient uptake of a rifampicin derivative via the FhuA-TonB-dependent uptake route in *Escherichia coli*. J. Gen. Microbiol. *133*, 3505–3511.
10. Kadner, R.J., Heller, K., Coulton, J.W., and Braun, V. (1980). Genetic control of hydroxamate-mediated iron uptake in *Escherichia coli*. J. Bacteriol. *143*, 256–264.
11. Locher, K.P., and Rosenbusch, J. (1997). Oligomeric states and siderophore binding of ligand-gated FhuA protein that forms channels across *Escherichia coli* outer membranes. Eur. J. Biochem. *247*, 770–775.
12. Bös, C., Lorenzen, D., and Braun, V. (1998). Specific *in vivo* labelling of cell surface-exposed protein loops: reactive cysteines in the predicted gating loop mark a ferrichrome binding site and a ligand-induced conformational change of the *Escherichia coli* FhuA protein. J. Bacteriol. *180*, 605–613.
13. Schöffler, H., and Braun, V. (1989). Transport across the outer membrane of *Escherichia coli* K12 via the FhuA receptor is regulated by the TonB protein of the cytoplasmic membrane. Mol. Gen. Genet. *217*, 378–383.
14. Moeck, G.S., et al., and Coulton, J.W. (1996). Ligand-induced conformational change in the ferrichrome-iron receptor of *Escherichia coli* K-12. Mol. Microbiol. *22*, 459–471.
15. Moeck, G.S., Coulton, J.W., and Postle, K. (1997). Cell envelope signalling in *Escherichia coli*: ligand binding to the ferrichrome-iron receptor FhuA promotes interaction with the energy-transducing protein TonB. J. Biol. Chem. *272*, 28391–28397.
16. Günther, K., and Braun, V. (1990). *In vivo* evidence for FhuA outer membrane receptor interaction with the TonB inner membrane protein of *Escherichia coli*. FEBS Lett. *274*, 85–88.
17. Buchanan, S.K., et al., and Deisenhofer, J. (1999). Crystal structure of the outer membrane active transporter FepA from *Escherichia coli*. Nat. Struct. Biol. *6*, 56–63.
18. Cadieux, N., and Kadner, R.J. (1999). Site-directed disulfide bonding reveals an interaction site between energy-coupling protein TonB and BtuB, the outer membrane cobalamin transporter. Proc. Natl. Acad. Sci. USA *96*, 10673–10678.
19. Merianos, H.J., Cadieux, N., Lin, C.H., Kadner, R.J., and Cafiso, D.S. (2000). Substrate-induced exposure of an energy-coupling motif of a membrane transporter. Nat. Struct. Biol. *7*, 205–209.
20. Braun, M., Killmann, H., and Braun, V. (1999). The β-barrel domain of FhuAΔ5–160 is sufficient for TonB-dependent FhuA activities of *Escherichia coli*. Mol. Microbiol. *33*, 1037–1049.
21. Bonhivers, M., Ghazi, A., Boulanger, P., and Letellier, L. (1996). FhuA, a transporter of the *Escherichia coli* outer membrane is converted into a channel upon the binding of bacteriophage T5. EMBO J. *15*, 1850–1856.
22. Plançon, L., Chami, M., and Letellier, L. (1997). Reconstitution of FhuA, an *Escherichia coli* outer membrane protein, into liposomes. Binding of phage T5 to FhuA triggers the transfer of DNA into the proteoliposomes. J. Biol. Chem. *272*, 16868–16872.
23. Killmann, H., Herrmann, C., Wolff, H., and Braun, V. (1998). Identification of a new site for ferrichrome transport by comparison of the FhuA proteins of *Escherichia coli*, *Salmonella paratyphi B*, *Salmonella typhimurium*, and *Pantoea agglomerans*. J. Bacteriol. *180*, 3845–3852.
24. Hartmann, G.R., et al., and Weiss, W. (1985). Molekulare wirkungsweise des antibioticums rifampicin. Angew. Chemie *97*, 1011–1017.
25. Schirmer, T., Keller, T.A., Wang, Y., and Rosenbusch, J.P. (1995). Structural basis for sugar translocation through maltoporin channels at 3.1 Å resolution. Science *267*, 512–514.
26. Forst, D., Welte, W., Wacker, T., and Diederichs, K. (1998). Structure of ScrY, the sucrose-specific porin from *Salmonella typhimurium*, and its complex with sucrose at 2.4 Å resolution. Nat. Struct. Biol. *5*, 37–46.
27. Kabsch, W. (1988). Evaluation of single crystal X-ray diffraction data from a position sensitive detector. J. Appl. Crystallogr *21*, 916–924.
28. Jones, T.A., Zou, J.Y., Cowan, S.W., and Kjeldgaard, M. (1991). Improved methods for building protein models in electron density maps and the location of errors in these models. Acta Crystallogr. A *47*, 110–119.
29. Brünger, A.T., et al., and Warren, G.L. (1998). Crystallography & NMR system: A new software suite for macromolecular structure determination. Acta Crystallogr. D *54*, 905–921.
30. Miller, J.H. (1972). Experiments in Molecular Genetics (New York: Cold Spring Harbor Laboratory Press).
31. Moeck, G.S., et al., and Coulton, J.W. (1994). Genetic insertion and exposure of a reporter epitope in the ferrichrome-iron receptor of *Escherichia coli* K-12. J. Bacteriol. *176*, 4250–4259.
32. Ferguson, A.D., Breed, J., Diederichs, K., Welte, W., and Coulton, J.W. (1998). An internal affinity-tag for purification and crystallization of the siderophore receptor FhuA, integral outer membrane protein from *Escherichia coli* K-12. Protein Sci *7*, 1636–1638.
33. Kraulis, P.J. (1991). MOLSCRIPT: a program to produce both detailed and schematic plots of protein structures. J. Appl. Crystallogr. *24*, 946–950.
34. Merrit, E.A., and Bacon, D.J. (1997). Raster3D photorealistic molecular graphics. Methods Enzymol. *277*, 505–524.

Accession Numbers

The crystallographic coordinates (FhuA in complex with rifamycin CGP 4832) and structure factor amplitudes have been deposited in the Protein Data Bank with the accession code 1FI1.